

Temperature and angular dependences of dynamic spin-polarized resonant tunneling in CoFeB/MgO/NiFe junctions

Casey W. Miller,^{1,a)} Ivan K. Schuller,² R. W. Dave,³ J. M. Slaughter,³ Yan Zhou,⁴ and Johan Åkerman⁴

¹Department of Physics, University of South Florida, 4202 E. Fowler Avenue, Tampa, Florida 33620 USA

²Department of Physics, University of California, San Diego, 9500 Gilman Drive, La Jolla, California 92093, USA

³Technology Solutions Organization, Freescale Semiconductor, Inc., 1300 North Alma School Road, Chandler, Arizona 85224, USA

⁴Department of Microelectronics and Applied Physics, Royal Institute of Technology, Electrum 229, 164 40 Kista, Sweden

(Presented on 9 November 2007; received 12 September 2007; accepted 19 October 2007; published online 7 February 2008)

The bias dependence of tunneling magnetoresistance oscillations due to dynamic resonant tunneling in CoFeB/MgO/NiFe magnetic tunnel junctions was studied as functions of temperature and the relative magnetization angle of the two magnetic layers. The effect of temperature is consistent with thermal smearing, while that of the relative magnetic orientation was typical of a spin valve. A model of tunneling between spin-split free electron bands using the exact solution of the Schrödinger equation for a trapezoidal tunnel barrier agrees with experiment, underscoring the simplicity of dynamic resonant tunneling. © 2008 American Institute of Physics.

[DOI: [10.1063/1.2831393](https://doi.org/10.1063/1.2831393)]

The technological applications of spin-dependent tunneling are profound.¹ The most pertinent example of this is magnetoresistive random access memory (MRAM), which combines nonvolatility, unlimited read/write cycles, high read and write speeds, and long-term reliability.^{2–4,24} While aluminum oxide (AlOx) has traditionally been the tunneling barrier of choice in magnetic tunnel junctions (MTJs), the continual reports of room temperature magnetoresistance increases beyond 400% in MgO-based MTJs with CoFeB ferromagnetic electrodes promise future improvements for MRAM and related technologies.^{5,6} Further, a significant read speed increase was indeed demonstrated in a 4 Mbit MRAM circuit with MgO tunnel barriers and NiFe/Ru/NiFe synthetic antiferromagnet (SAF) free layers.⁷ To complement these advances, the realization of dynamic spin-polarized resonant tunneling in CoFeB/MgO/NiFe tunnel junctions may be a novel route to tune the performance of tunneling devices.⁸ Here, we describe the dependence of the well defined and reproducible oscillations observed in CoFeB/MgO/NiFe magnetic tunnel junctions as functions of temperature and the relative angle between the magnetizations of the pinned CoFeB and the free NiFe. Other oscillatory behavior has been studied in magnetic tunneling as well.^{9–11}

The MTJs used in this study were composed of pinned CoFe/Ru/CoFeB SAFs, MgO tunneling barriers, and free NiFe-based SAFs; specific details have been described previously.^{7,12} All devices satisfied the MTJ tunneling criteria,^{13,25} proving that tunneling is the primary conduction mechanism. At the wafer level, room temperature *I-V* characteristics were measured on 26 MTJs using a source-meter

unit, from which differential resistance (dV/dI) data were obtained by numerical differentiation. After wafer dicing and packaging devices into chip carriers, direct dV/dI measurements were made on 29 different junctions between 5 and 300 K using a high resolution resistance bridge with standard lock-in techniques. The data from these two methods quantitatively agreed. The dc bias was applied to the NiFe free layer with the CoFeB pinned layer grounded in all measurements. The observed behavior was independent of bit shape and area, which varied from 1100×420 nm² ellipses to 600 nm–10 μ m diameter circles. For succinctness, data presented are from 600 nm circular bits. We define the dMR at a given temperature quite generally as

$$dMR(\theta) = \frac{dV/dI(\theta) - dV/dI_p}{dV/dI_p}, \quad (1)$$

where θ is the angle between the free and pinned magnetizations, and dV/dI_p is the differential resistance in the parallel state; the antiparallel differential resistance (dV/dI_{ap}) is given by $dV/dI(180^\circ)$.

Figure 1(a) shows the experimental bias dependence of the differential junction magnetoresistance (dMR) measured at 5 and 300 K. The most striking features of these data are that the dMR becomes negative and oscillates about zero when electrons tunnel from CoFeB into NiFe (i.e., positive bias). After changing sign at 0.67 V, the dMR has a peak negative value of -8% , followed by a $+5\%$ positive peak at 1.4 V, and approaches zero near 1.8 V. Additionally, dMR becomes negative for negative biases more negative than -1.5 V. This negative dMR region for negative biases indicates the onset of the oscillatory behavior, though full oscillations cannot be observed due to dielectric breakdown of the devices at high biases. The barrier height ϕ at the collector

^{a)}Electronic mail: cmiller@cas.usf.edu.

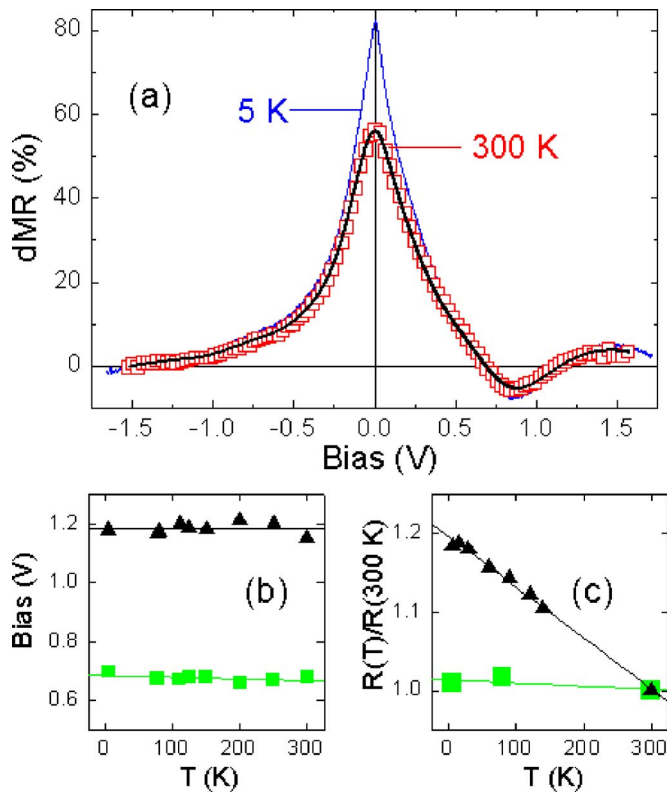


FIG. 1. (Color online) (a) Bias dependence of the experimental differential magnetoresistance of CoFeB/MgO/NiFe MTJs at 5 K (thin blue line) and 300 K (red squares), along with a thermal smearing fit of the 300 K data (thick black line). (b) The first (green squares) and second (black triangles) positive bias zero crossings were independent of temperature. (c) Temperature dependence of the zero-bias resistance in the parallel (green squares) and antiparallel (black triangles) states normalized to the room temperature value for each state. Lines are linear fits to the data in both (b) and (c).

interface defines the threshold for these oscillations,⁸ so one may infer that ϕ is larger for the CFB–MgO interface than for the NiFe–MgO interface. This is indeed corroborated by barrier heights extracted from the conductance data via both the model of Brinkman *et al.*¹⁴ ($\phi_{\text{CFB–MgO}}=2.7$ eV, $\phi_{\text{NiFe–MgO}}=1.5$ eV), and the model developed to describe dynamic resonant tunneling ($\phi_{\text{CFB–MgO}}=1.2$ eV, $\phi_{\text{NiFe–MgO}}=0.6$ eV). The zero-crossing biases (i.e., the bias for which $dMR=0$) were independent of temperature [Fig. 1(b)], while the zero-bias dV/dI in the parallel and antiparallel magnetic configurations [Fig. 1(c)] had the typical temperature dependence expected for tunneling devices.¹³

The differences between the 5 and 300 K device characteristics are consistent with thermal smearing.^{15,16} We assume Bloch's law $T^{3/2}$ temperature dependence of the surface polarization of each tunnel junction interface. For simplicity we model the combined effect of the two interfaces as a single temperature-dependent spin polarization, $P(T)=P_0(1-\alpha T^{3/2})$,¹⁷ where α is a free fitting parameter. The second free parameter is an effective electron temperature T^* in the Fermi-Dirac distribution of the tunneling electrons. We use the dMR data at 5 K as an approximation to device characteristics at absolute zero temperature, and convolute these data with the Fermi-Dirac distribution evaluated at T^* . The resulting curve is scaled by $P(T)$ and finally compared with the actual dMR data at 300 K. A standard least-squares ap-

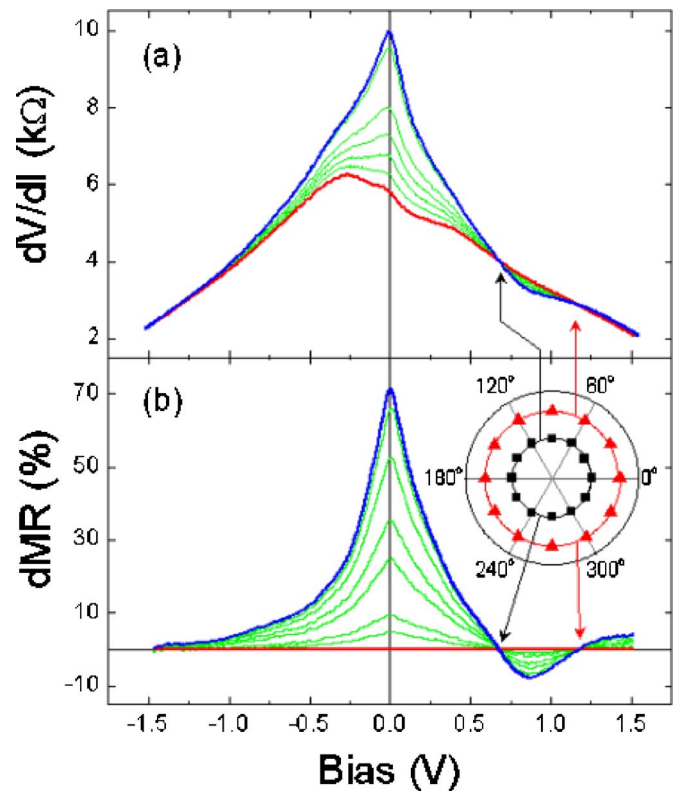


FIG. 2. (Color online) (a) Bias dependence of differential resistance (dV/dI) in CoFeB/MgO/NiFe MTJs at 125 K for several representative applied field angles. The dV/dI changed systematically from the antiparallel state (top curve, blue) to the parallel state (bottom curve, red) as the magnetic orientation was changed between these states using the applied in-plane field. (b) Bias dependence of the differential junction magnetoresistance obtained from the dV/dI data in (a) via Eq. (1). (Inset) The first (squares) and second (triangles) zero crossings (+0.68 and +1.19 V, indicated by the arrows) were independent of angle.

proach is then used to minimize the χ^2 error with respect to T^* and α . Figure 1(a) shows a fit (black line) of experimental 300 K dMR data (symbols) with this procedure using $\alpha=3.85\times 10^{-5}\text{ K}^{-3/2}$ [i.e., $P(300\text{ K})/P(5\text{ K})=0.8$] and an effective temperature for thermal smearing of $T^*=440$ K. The relatively high α ($\alpha_{\text{NiFe}}=1.23\times 10^{-5}\text{ K}^{-3/2}$ in the bulk¹⁸) is consistent with previously reported values of $(3-5)\times 10^{-5}\text{ K}^{-3/2}$ for MTJs with a NiFe free layer.¹⁷ The higher than expected smearing temperature, $T^*/T_{\text{exp}}=1.5$, is consistent with earlier reports where $T^*/T_{\text{exp}}=1.6$. This discrepancy originates from neglecting a term in the smearing equations, but the experimental device temperature is recovered when that term is included.¹⁵

To investigate the angular dependence, a 50 G in-plane field was used to define the relative angle between the magnetizations of the NiFe and CoFeB. The magnetization of the NiFe free layer is approximately parallel to the applied field, while that of the CoFeB is nearly independent of such a perturbative field, thus allowing the relative magnetic orientation of the free and pinned layers to be controlled externally. Figure 2(a) shows how the relative angle between the two magnetizations affects the bias dependence of the differential resistance at 125 K. The dV/dI data evolve systematically from the parallel to antiparallel configurations (and *vice versa*). To investigate the oscillations in more details, the

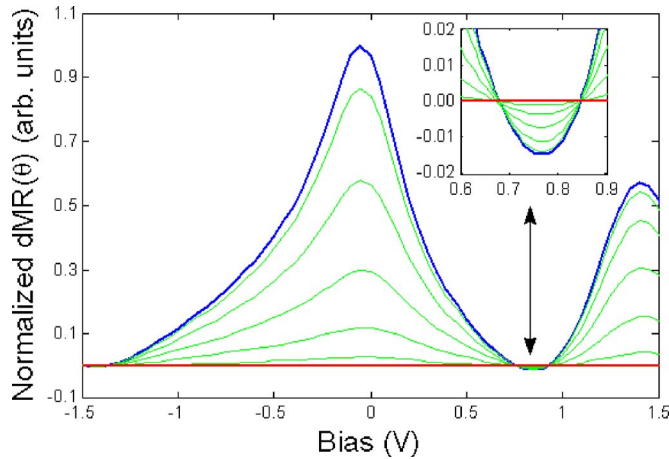


FIG. 3. (Color online) Model calculations of the bias dependence of the normalized differential junction magnetoresistance for several applied field angles (θ) qualitatively reproduce the experimental dMR of Fig. 2(b). The field angle was simulated by varying the polarization of one electrode as $(1 + \cos \theta)/2$ in 30° steps. The antiparallel state is the top curve (blue), and the parallel state is the horizontal (red) curve where dMR is zero. (Inset) The first and second positive bias zero crossings were independent of angle.

dMR was calculated from these dV/dI data according to Eq. (1). Figure 2(b) shows that the angle of the applied field reduces the dMR magnitude, but it does not affect the zero crossings or oscillation period. The inset of Fig. 2 shows that the first and second zero crossings were independent of the angle between the free and pinned magnetic layers. While the spin dependence of the reflection coefficient at the collector interface is mediated by the spin bottleneck (resulting in the larger amplitude of the AP state than the P state), the phase of the reflected wave function is independent of spin. Thus, the zero crossings have no explicit angular dependence.

One possible explanation for this oscillatory bias dependence is electron interference within the barrier.^{8,19} In the Fowler-Nordheim (FN) tunneling regime, the incident electron energy exceeds the potential barrier near the collector, allowing electrons to tunnel directly into the conduction band of the insulator. These electrons have real kinetic energy *within the barrier* and can thus be treated as plane waves. Incident and reflected electrons may then interfere and establish standing waves in the region of the barrier where the energy of the electron is real. The experimentally observed bias dependence is qualitatively reproduced by exactly solving the Schrödinger equation for a trapezoid tunnel barrier with spin-split free electron bands representing the ferromagnetic electrodes.⁸ This formalism includes material dependent effective masses, which were taken to be $m^* = 1.3m_e$ for both ferromagnets,²⁰ and $0.4m_e$ for the MgO barrier.²¹ The polarizations (P) of CoFeB and NiFe were assumed to be 55% and 45%.^{22,23} The dependence of the tunneling current on the angle between the free and pinned layers was simulated by varying the NiFe polarization as $P_{\text{NiFe}}(\theta) = 45\% \times (1 + \cos \theta)/2$. Figure 3 shows that model calculations qualitatively reproduce the experimental angular dependence of both the dMR and the nodal behavior of the zero-crossings. Discrepancies in the amplitude are attributed to imperfections such as interface roughness.²⁶

In summary, bias-dependent oscillations associated with dynamic resonant tunneling were observed in the differential resistance of CoFeB/MgO/NiFe magnetic tunnel junctions. The temperature dependence of the data was consistent with thermal smearing, while the dependence on the relative magnetization angle was consistent with spin-valve behavior. Neither parameter significantly affected the oscillatory behavior. A coherent tunneling model using the exact solution of the Schrödinger equation and spin-split free electrons representing the ferromagnets qualitatively reproduced the angular dependence, underscoring the simplicity of the spin-polarized dynamic resonant tunneling phenomenon.

Supported by the US DOE (UCSD), the Swedish Foundation for Strategic Research, The Swedish Research Council, and The Göran Gustafsson Foundation (J.Å.). The authors thank Z.-P. Li and D. Mix for assistance.

- ¹M. Johnson, *Magneto-electronics* (Elsevier, Oxford, 2004).
- ²J. Åkerman, P. Brown, M. DeHerrera, M. Durlam, E. Fuchs, D. Gajewski, M. Griswold, J. Janesky, J. Nahas, and S. Tehrani, *IEEE Trans. Device Mater. Reliab.* **4**, 428 (2004).
- ³B. N. Engel, J. Åkerman, B. Butcher, R. W. Dave, M. DeHerrera, M. Durlam, G. Grynkeiwich, J. Janesky, S. V. Pietambaram, N. D. Rizzo, J. M. Slaughter, K. Smith, J. J. Sun, and S. Tehrani, *IEEE Trans. Magn.* **41**, 132 (2005).
- ⁴J. Åkerman, P. Brown, D. Gajewski, M. Griswold, J. Janesky, M. Martin, H. Mekonnen, J. J. Nahas, S. Pietambaram, J. M. Slaughter, and S. Tehrani, 2005 IEEE International Reliability Physics Symposium, Chandler, AZ.
- ⁵S. Yuasa, A. Fukushima, H. Kubota, Y. Suzuki, and K. Ando, *Appl. Phys. Lett.* **89**, 042505 (2006).
- ⁶S. Ikeda, J. Hayakawa, Y. M. Lee, F. Matsukura, and H. Ohno, *J. Magn. Mater.* **310**, 1937 (2006).
- ⁷R. W. Dave, G. Steiner, J. Slaughter, B. Craigo, S. Pietambaram, K. Smith, G. Grynkeiwich, M. DeHerrera, J. Åkerman, and S. Tehrani, *IEEE Trans. Magn.* **42**, 1935 (2006).
- ⁸C. W. Miller, Z.-P. Li, I. K. Schuller, R. W. Dave, J. M. Slaughter, and J. Åkerman, *Phys. Rev. Lett.* **99**, 047206 (2007).
- ⁹Y. Ren, Z.-Z. Li, M.-W. Xiao, and A. Hu, *J. Phys.: Condens. Matter* **17**, 4121 (2005).
- ¹⁰M. Sharma, S. X. Wang, and J. H. Nickel, *Phys. Rev. Lett.* **82**, 616 (1999).
- ¹¹E. Y. Tsymlal, A. Sokolov, I. F. Sabirianov, and B. Doudin, *Phys. Rev. Lett.* **90**, 186602 (2003).
- ¹²C. W. Miller, Z.-P. Li, I. K. Schuller, R. W. Dave, J. M. Slaughter, and J. Åkerman, *Phys. Rev. B* **74**, 212404 (2006).
- ¹³J. J. Åkerman, J. M. Slaughter, R. W. Dave, and I. K. Schuller, *Appl. Phys. Lett.* **79**, 3104 (2001).
- ¹⁴W. F. Brinkman, R. C. Dynes, and J. M. Rowell, *J. Appl. Phys.* **41**, 1915 (1970).
- ¹⁵J. J. Åkerman, I. V. Roshchin, J. Slaughter, R. W. Dave, and I. K. Schuller, *Europhys. Lett.* **63**, 104 (2003).
- ¹⁶I. Schuller, R. Orbach, and P. M. Chaikin, *Phys. Rev. Lett.* **41**, 1413 (1978).
- ¹⁷C. H. Shang, J. Nowak, R. Jansen, and J. S. Moodera, *Phys. Rev. B* **58**, R2917 (1998).
- ¹⁸D. Scholl, M. Donath, D. Mauri, E. Kay, J. Mathon, R. B. Muniz, and H. C. Siegmann, *Phys. Rev. B* **43**, 13309 (1991).
- ¹⁹K. H. Gundlach, *Solid-State Electron.* **9**, 949 (1966).
- ²⁰A. H. Davis and J. M. MacLaren, *J. Appl. Phys.* **87**, 5224 (2000).
- ²¹W. H. Butler, X.-G. Zhang, T. C. Schulthess, and J. M. MacLaren, *Phys. Rev. B* **63**, 054416 (2001).
- ²²R. Wang, X. Jiang, R. M. Shelby, R. M. Macfarlane, S. S. P. Parkin, and J. S. Harris, *Appl. Phys. Lett.* **86**, 052901 (2005).
- ²³D. J. Monsma and S. S. P. Parkin, *Appl. Phys. Lett.* **77**, 720 (2000).
- ²⁴J. Åkerman, *Science* **308**, 508 (2005).
- ²⁵B. J. Jönsson-Åkerman, R. Escudero, C. Leighton, S. H. Kim, I. K. Schuller, and D. Rabson, *Appl. Phys. Lett.* **77**, 1870 (2000).
- ²⁶C. W. Miller, Z.-P. Li, J. Åkerman, and I. K. Schuller, *Appl. Phys. Lett.* **90**, 043513 (2007).